JOURNAL OF MATERIALS SCIENCE 16 (1981) 957–967

Study of the structure and crystallization of an Fe–17 at % B amorphous alloy

K. OSAMURA, K. SHIBUE, R. SUZUKI, Y. MURAKAMI
Department of Metallurgy, Kyoto University, 606 Kyoto, Japan

S. TAKAYAMA
Central Laboratory, Hitachi Ltd, 185 Kokubunji, Tokyo, Japan

The structure of an $Fe_{83}B_{17}$ amorphous alloy was examined in detail, mainly by means of small-angle X-ray scattering (SAXS) measurements. The electron density–density correlation derived from the observed intensity had the following characteristic features: a strong correlation concentrated in the short radial distances within about 1.2 nm and a rather weak correlation towards larger distances. After quantitative analysis, it was concluded that a compositional fluctuation occurs on a fine scale of about 1 nm in the amorphous Fe–B alloys, even though phase separation is not present as completely as in the structure model proposed by Boudreaux. Electrical resistivity measurements as well as transmission electron microscope (TEM) observations were performed to investigate the crystallization process. By using the theoretical equation of electrical resistivity reported by Landauer, the temperature dependence for the partially aged amorphous alloys was analysed. The volume fraction of crystalline phase estimated from the present analysis was in good agreement with the results obtained from TEM observation.

1. Introduction

Even if it is ambiguous, a deviation from statistical randomness on an atomic arrangement can often be found in an amorphous phase. Up to now, extensive information, mainly on nearest neighbours, has been accumulated by several experimental techniques. However, less structural information has been reported concerning larger separations in space. One of the techniques available to obtain such long-distance information is small-angle X-ray scattering (SAXS). In a recent report, we showed that there exists an electron density fluctuation over the order of several nanometers in an Fe–P–C amorphous alloy [1]. This fluctutation might originate from two alternative kinds of structural inhomogeneities. One is a composition fluctuation, which means a growth of molecular cluster-like zones in metallic alloys, or a spinodal decomposition. In this case, a rearrangement of metalloid atoms is essential. Another kind of inhomogeneity arises when small close-packed or local ordered regions are mixed in less close or ordered regions, and an electron density fluctuation can be expected. Here the packing manner of the metallic atoms plays an important role.

Recently, Boudreaux [2] discussed the structure of metallic glass alloys. In the Fe–B system, he suggested that the metalloid is a centre of a molecular unit with a fixed structure that depends on the nature of the transition metal–metalloid interaction. The units pack together to form a glass structure, and the extra transition metal atoms fill the space between units. This is in agreement with the idea of Gilman [3] who argues that such molecular units exist in a liquid state near the eutectic composition. An investigation using Mössbauer spectroscopy by Kemény *et al.* [4] supported the above theoretical consideration. They concluded that a quasi-crystalline model, based on the metastable Fe_3B intermetallic compound, satisfactorily described their main experimental observation. Using the quasi-crystalline model, other physical properties, such as density

0022–2461/81/040957–11$03.10/0

[5], magnetic moment of Fe atoms [6], thermal expansion [7] and nearest-neighbour co-ordination number [8] can be well explained.

In the present work, we carried out SAXS measurements as well as transmission electron microscope (TEM) observations and electrical resistivity measurements on an Fe–17 at% B alloy. These results were analysed in order to obtain structural information on the amorphous state and its crystallization process.

2. Experimental method

An amorphous Fe–B alloy was made by a single-side drum technique. Long ribbons about 25 μm thick and 5 mm wide were obtained. The nominal chemical composition was Fe–17 at% B. For TEM observation, the specimens were electrolytically thinned in an electrolyte consisting of 10% perchloric acid and 90% ethyl alcohol. The temperature of the electrolyte was kept at $-5°$ C or lower. The thinned specimens were examined in a JEOL-120 transmission electron microscope. The TEM observations were performed on the same specimens used for X-ray measurements.

SAXS measurements were performed in transmission geometry with a Kratky camera, as detailed in our previous report [1]. Molybdenum radiation was generated by a Rigaku RU200PL power supply operated at 50 kV and 160 mA. The scattering intensity from the foil of fully annealed pure Fe was adopted as the background intensity after absorption correction. In order to check the structural change during isothermal ageing, the diffraction intensity was measured over a wide range of scattering angles, using an ordinary 2θ–θ diffractometer in transmission geometry.

The change of electrical resistivity was measured during two kinds of heat treatment: isothermal ageing and heating and cooling at a constant rate. High-purity Al wires were spot-welded on to a long ribbon of amorphous alloy and the specimen put into a fused silica ampoule filled with He gas. The direct current electrical resistivity was measured at the desired temperatures.

3. Experimental results and discussion

3.1. Crystallization

Fig. 1 shows the change of electrical resistivity during isothermal ageing at 595 and 546 K. The onset of a large decrease in resistivity occurred at about 60 ksec and 1 Msec at 595 and 546 K, respectively. Before the large decrease, however, a small slow change appeared in $\Delta\rho/\rho$. The electrical resistivity for the amorphous alloy before ageing was 1760 and 1710 nΩ m at 300 and 77 K, respectively.

The structure change was observed by TEM. Fig. 2 shows a typical structure which appeared during ageing at 595 K. For an as-received specimen, the bright-field image (Fig. 2a) shows a

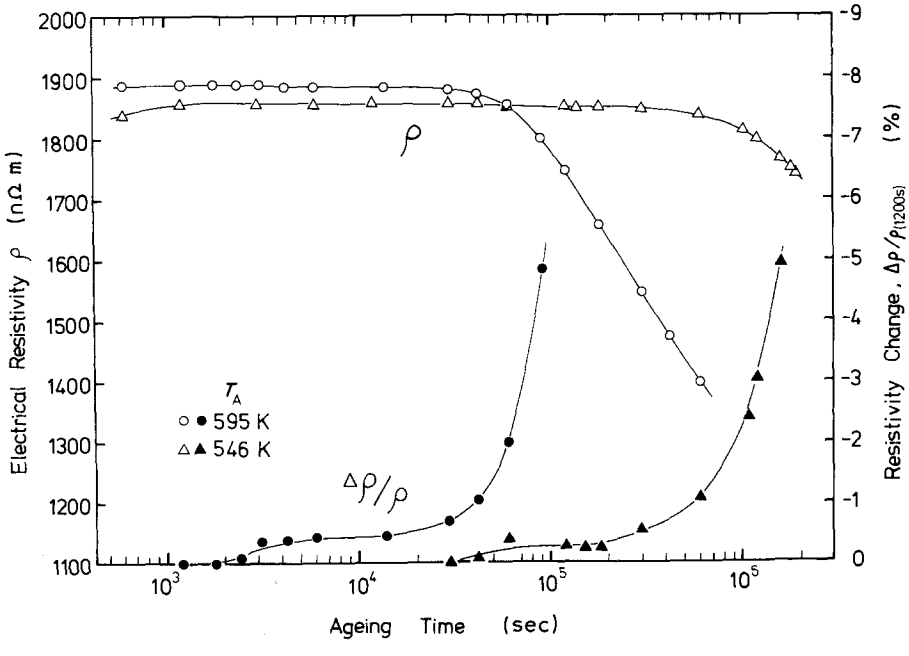

Figure 1 Dependence of electrical resistivity on ageing time for an amorphous Fe–17 at % B alloy.

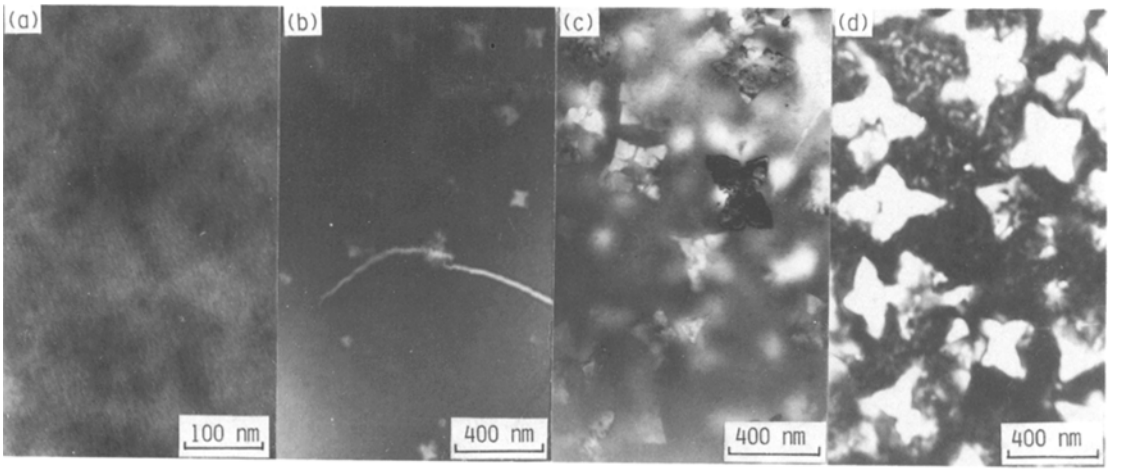

Figure 2 Change in structure of an amorphous Fe–17 at % B alloy aged at 595 K for various times. (a) As-received, (b) 60 ksec, (c) 300 ksec, (d) 6 Msec.

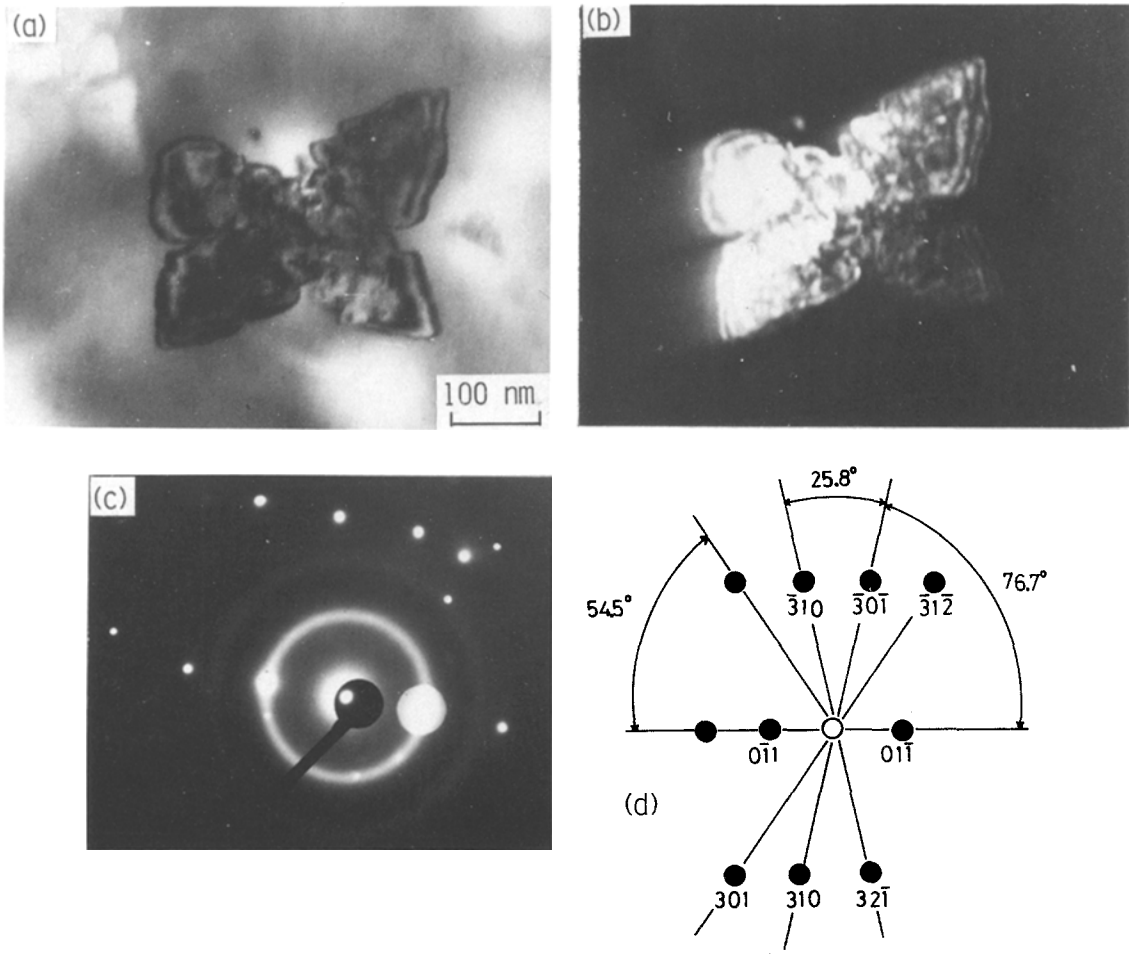

Figure 3 Crystalline particle in Fe–B alloy aged at 595 K for 300 ksec. (a) Bright-field image, $B = [\bar{1}33]_\alpha$, (b) dark-field image using $(01\bar{1})_\alpha$ spot, (c) selected-area diffraction pattern, (d) diagram showing b c c crystalline structure $B = [133]_P$.

typical "pepper and salt" background structure and only broad halo rings are observed in the selected-area diffraction pattern (SADP). Crystalline phases appear clearly in the specimen aged for 60 ksec, the average size of the crystalline particles being about 50 to 100 nm. Their size increased during ageing, but the density of particles did not apparently increase. As shown in Fig. 2d, not all of the amorphous phases aged at 595 K transformed completely into a crystalline phase even after 6 Msec ageing. When the alloy was aged at 546 K, similar crystalline particles, as shown in Fig. 2b, were observed for the specimen aged for 600 ksec. Fig. 3 shows the results of structural analyses of these crystalline particles. The SADP consists of halos originating from an amorphous matrix and a set of sharp spots from crystalline phase. These sharp spots are indexed as belonging to α-Fe, as shown in the key diagram reported by Walker *et al.* [9]. Dark-field imaging using the $(01\bar{1})_\alpha$ spot indicates that the phase is not a single crystal, but irregular in shape.

The temperature dependence of electrical resistivity was measured for the specimen aged at 595 K for an appropriate period, during which crystalline particles precipitated. The heating and cooling rates were 0.0315 and 0.0235 K sec^{-1}, respectively. As shown in Fig. 4, the resistivity during heating increased gradually at first, decreased rapidly beyond about 600 K and then fell towards a constant value around 702 K. As is well known, the rapid decrease is due mainly to crystallization. For a specimen aged for a longer period, the resistivity became smaller and its temperature dependence larger. The diamond signs in the figure show the resistivity just after the respective ageing; this was consistent with the value observed during the following heating from room temperature. This means that no structural change occurred at least up to 595 K during the present handling. After crystallization, the resistivity change during cooling was similar for all specimens except for the case of 600 ksec ageing.

Landauer [10] has given an expression for the electrical resistivity of a two-phase metallic mixture, based on the classical electromagnetic theory:

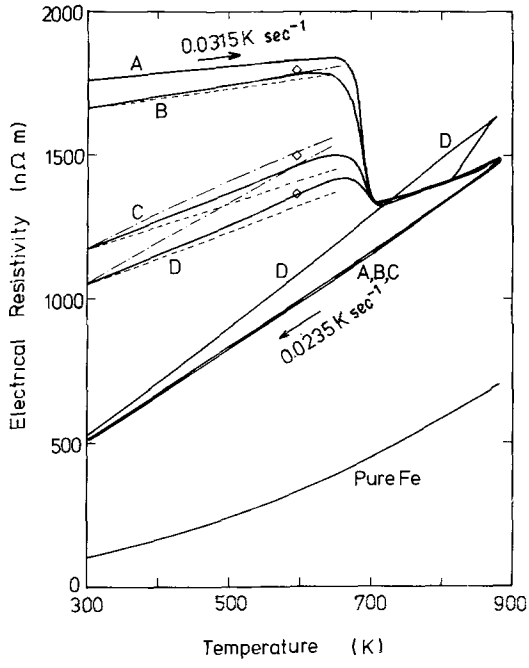

Figure 4 Change of electrical resistivity as a function of temperature. A, the as-received specimen; B, C and D, specimens aged at 595 K for 60, 300 and 600 ksec, respectively. The two curves (–·–·– and --------) are theoretically calculated by assuming the terminal value of ρ_2 as being the resistivity after crystallization and that of pure Fe, respectively.

where ρ_m is the resistivity of the mixture, V_1 and V_2 are the fractions of the total volume occupied by Phases 1 and 2 respectively ($V_1 + V_2 = 1$), and ρ_1 and ρ_2 are the respective resistivities. The ratio of volume fractions is expressed by the equation

$$\frac{V_1}{V_2} = \frac{(\rho_m - \rho_2)(\rho_m + 2\rho_1)}{(\rho_1 - \rho_m)(\rho_m + 2\rho_2)}. \quad (2)$$

Here Phase 1 is the amorphous phase and the resistivity ρ_1 corresponds to that of the as-received sample. Phase 2 is a crystalline phase after crystallization and the values of the resistivity ρ_2 are assumed to be those shown by the cooling curve as shown in Fig. 4. The resistivity measured at 300 K is shown in Table I. By using Equation 2, the volume fraction occupied by the crystalline phase was estimated for the sample aged at 595 K.

Similarly, the resistivity at other temperatures can be calculated by putting ρ_1, ρ_2 and V_2 into

$$\rho_m = \frac{4\rho_1}{(3V_2 - 1)(\rho_1/\rho_2) + 3V_1 - 1 + \{[3V_2 - 1)(\rho_1/\rho_2) + 3V_1 - 1]^2 + (8\rho_1/\rho_2)\}^{1/2}}, \quad (1)$$

TABLE I Electrical resistivity of Fe–17 at % B alloys at 300 K and the volume fraction V_2 of the crystalline phase deduced from the present analysis using Equation 2, where the alloys were aged at 595 K for the time indicated

Sample	$\rho_{300\,K}$ (nΩ m)	V_2*	V_2†
As-received	1760	0	0
After crystallization	518	1	–
Pure Fe [11]	101	–	1
After ageing for:			
6×10^4 sec	1662	0.04	0.02
3×10^5 sec	1169	0.29	0.14
6×10^5 sec	1045	0.37	0.17

*Terminal value ρ_2 taken as the resistivity after crystallization.
†Terminal value ρ_2 taken as that of pure Fe.

Equation 1, and is shown by chain-dotted lines in Fig. 4. The calculated value is larger than that from the experimental data. The discrepancy seems to originate from the following two reasons: first, the theory is based on the assumption that each phase is spherical and acts as if surrounded by a homogeneous medium whose properties are an average of the mixture. In the present case, however, the crystalline particles are not spherical in shape and are always surrounded by a continuously distributed amorphous phase. Secondly, we chose the resistivity after crystallization as the terminal value, ρ_2. The value may be larger than the specific resistivity of the primary crystallized α-Fe particles because the structure after crystallization consists of fine particles of α-Fe, Fe_2B and/or Fe_3B phases. Essentially, the terminal resistivity ρ_2 should be chosen to be that of an Fe–B solid solution with the α-Fe crystal structure.

Therefore, the temperature dependence of the resistivity was recalculated by assuming the resistivity of pure iron [11] as the terminal value, ρ_2. The result is shown by the dotted lines in Fig. 4 and is found to be smaller than the experimental data. It is suggested that the correct value of resistivity for the crystalline particles is intermediate between the two terminal resistivities mentioned above. By comparison with the photographs of Fig. 2b and c, the evaluated values in Table I appear to be reasonable in magnitude. By using Equation 1, it is possible to determine the resistivity of crystalline particles when the volume fraction is quantitatively obtained from TEM observation.

The angular dependence of SAXS intensity for the specimens aged at 595 K is shown in Fig. 5. It should be noted that a weak scattering intensity is observed for the as-received specimen. When small crystalline particles appeared, as shown in Fig. 2, a large SAXS intensity was observed, for example, for the specimens aged for 30 ksec or longer periods. The Guinier radius was measured to be 6.6 and 10.7 nm for 30 ksec and 6 Msec ageing at 595 K, respectively.

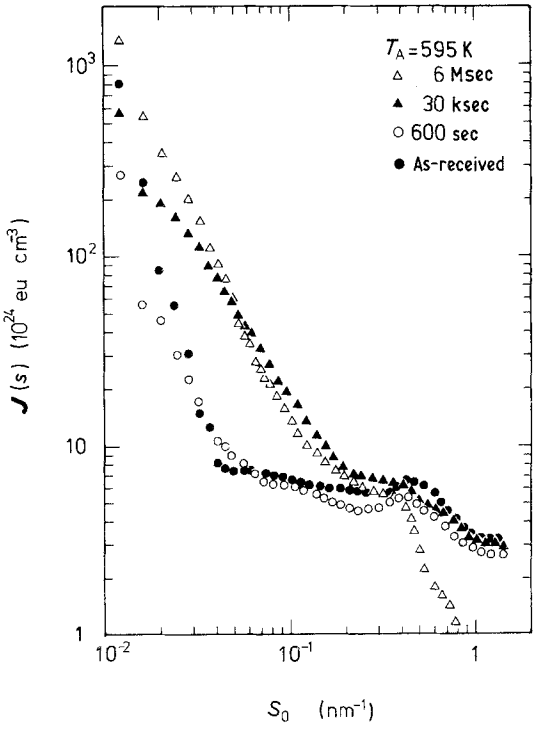

Figure 5 Angular dependence of SAXS intensity for the Fe–B amorphous alloys aged at 595 K, where s_0 is inverse Bragg spacing.

From the examination of stereo pairs of electron micrographs, Walter *et al.* [9] suggested that the size of α-Fe crystals grown at an early stage of crystallization is 40 to 70 nm across for $Fe_{73}Co_{10}B_{17}$ alloys, but that their thickness is very thin. In the present work, as shown in Fig. 3, primary crystals have grown in segments and do not show any twinning relationship with respect to each other. The size was 100 to 300 nm across in the specimen aged at 595 K for 6 Msec. From SAXS measurement, the Guinier radius was 10.7 nm. The Guinier radius is a kind of radius of gyration and hence gives much information about the smallest dimension in the case of irregular particles. Therefore, twice the observed Guinier radius seems to indicate the thickness of the α-Fe crystalline phase.

As discussed in our previous paper [1], the SAXS intensity is a function of the fluctuation of electron density in the material. The integrated intensity is defined as

$$\gamma(0) = \frac{\tau}{8\pi^3}\int_{s_i}^{s_f} 2\pi s \mathbf{J}(s)\, ds, \qquad (3)$$

where $\mathbf{J}(s)$ is a smeared intensity expressed in terms of absolute units, τ is a geometrical factor and s is expressed as $s = 2\pi s_0$, where s_0 is an inverse Bragg spacing. The limits of integration should theoretically be taken as $s_i = 0$ and $s_f = \infty$. In the present work, however, the integration was carried out from $s_i = 0.077\,\text{nm}^{-1}$ to $s_f = 3.0\,\text{nm}^{-1}$ owing to the experimental limitations.

Fig. 6 shows the change of integrated intensity during isothermal ageing. For the sample isothermally aged at 595 K, the intensity starts to increase at 1 to 10 ksec. Its increase is fairly consistent with the onset of the small decrease in the resistivity shown in Fig. 1 where no small crystalline particles were found from TEM observation. Thus this small increase in the integrated intensity appears to be a structural change in the amorphous matrix preceding the nucleation of α-Fe crystals.

3.2. Structure of amorphous phase

When an Fe–17 at% B amorphous alloy was aged at 546 K, the precipitation of crystalline particles was remarkably retarded in comparison with the case of 595 K ageing. The resistivity did not change appreciably up to 300 ksec. TEM observation showed that crystalline particles precipitate beyond 400 ksec. Fig. 7 is the result of large-angle X-ray diffraction measurements. The first and second peaks are diffuse which is usually recognized to be an indication of the amorphous state. The diffraction profile for the specimen aged for 300 ksec is very similar to that of the as-received specimen. After ageing for 600 ksec, the half-width of the first peak becomes narrower by a few per cent. For the 1.92 Msec aged specimen, the first peak sharpens, superimposed by the {110} Bragg diffraction of α-iron crystals.

Even in the amorphous state, a discernible change in SAXS intensity was observed during isothermal ageing at 546 K, as shown in Fig. 8. The intensity increases after ageing for a short period. The angular dependence of intensities for specimens aged up to 300 ksec is similar for each case. The large scattering intensity of the 1.92 Msec aged specimen results from the precipitation of crystalline particles.

The change in integrated intensity during ageing at 546 K is shown in Fig. 6. Following an increase after short ageing periods, the intensity decreases gradually up to $\sim 10^6$ sec, at which time the intensity rapidly increases, corresponding to the precipitation of crystalline particles. A correlation function, $\gamma(r)$, is calculated from the equation

$$\gamma(r) = \frac{1}{2\pi^2 r}\int_0^\infty sI(s)\sin(sr)\, ds, \qquad (4)$$

where $I(s)$ is the de-smeared intensity. A typical change of correlation function during ageing of

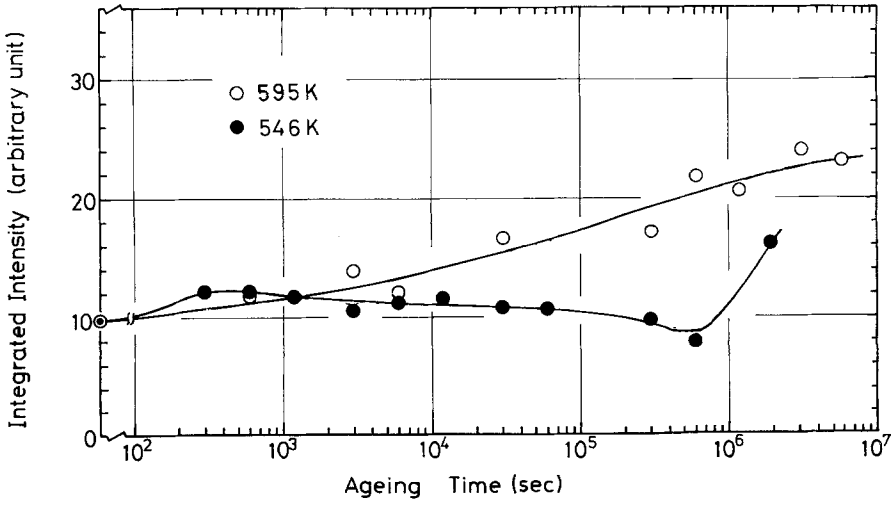

Figure 6 Dependence of the relative integrated intensity on ageing time.

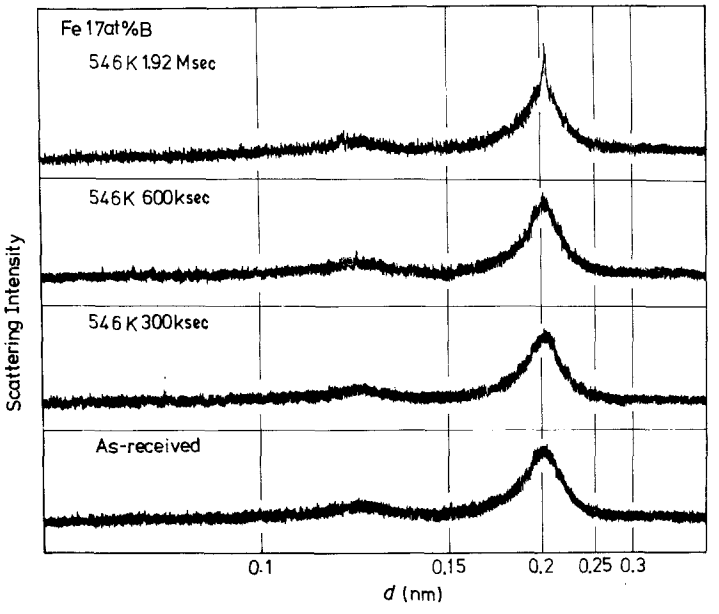

Figure 7 Wide-angle diffraction patterns as a function of Bragg spacing for the Fe–B alloys aged at 595 K.

an amorphous phase prior to crystallization is shown in Fig. 9. In general, the correlation function has two characteristics. One is the strong and rapidly decreasing correlation around the origin. The radial distance corresponding to zero correlation can be determined by extrapolating the slope near the origin. The value thus measured is 1.2 nm for the as-received specimen, while it remains nearly constant, i.e., 0.9 to 1.0, for the aged specimens, as listed in Table II. The other characteristic feature is the rather weak long-distance correlation, which seems to result from a correlation among the small scattering regions contributing to the SAXS intensity.

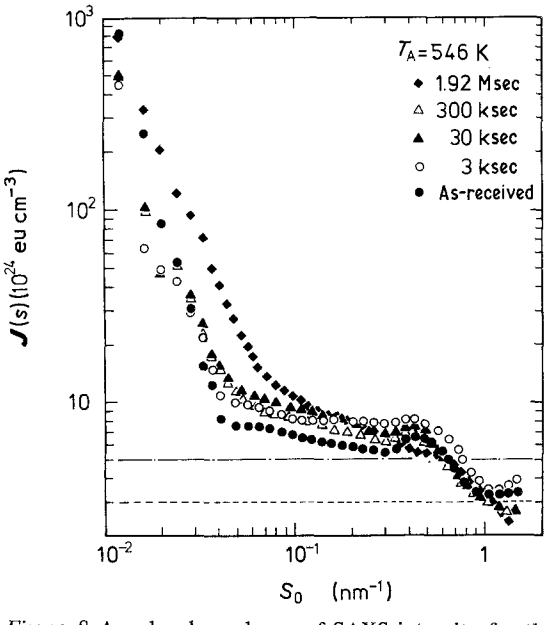

Figure 8 Angular dependence of SAXS intensity for the Fe–B amorphous alloys aged at 546 K. The two horizontal lines show the contribution from Laue monotonic scattering, the upper line is for a hypothetic supersaturated Fe–B alloy and the lower one indicates the expected monotonic scattering intensity from amorphous alloys.

Let us try to quantitatively analyse the result shown in Fig. 9. As a first approximation, it is reasonable that the small region of electron density fluctuation mentioned above is equiaxed or spherical. As discussed in the Appendix, the correlation function per unit volume is given by

$$\gamma(\mathbf{r}) = N\int_v \Delta\rho(r_1)\,\Delta\rho(r_1+r)\,\mathrm{d}r_1 + \sum_k \sum_{j\neq k} \int_v \Delta\rho(r_{k1})\,\Delta\rho(r_{k1}+r+R_k-R_j)\,\mathrm{d}r_{k1}. \quad (5)$$

The first term is the intra-particle correlation within each particle and the second term shows an inter-particle correlation among different particles. However, it is difficult to solve the above equation analytically without any information concerning a structural model. The relative position among particles, $R_k - R_j$, is usually an unknown factor. As shown in Equation 5, the correlation function only provides information in the vector space of $\Delta\rho(r)$. So a reasonable structure for the amorphous state must be deduced from the observed correlation. Here a simple one-dimensional model is proposed in order to understand the observed correlation shown in Fig. 9.

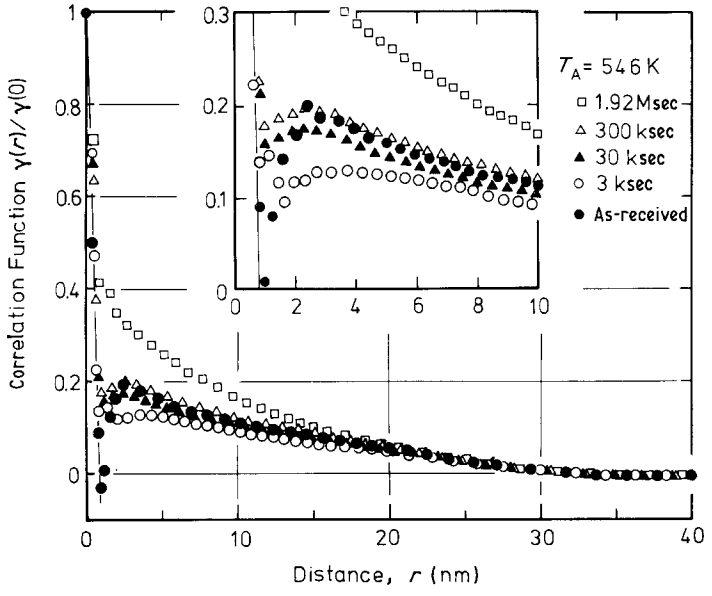

Figure 9 Relative density–density correlation function as a function of radial distance for the Fe–B amorphous alloys aged at 546 K.

A one-dimensional, reduced-structure model for the amorphous phase is shown in Fig. 10a. The central region is assumed to have a rectangular shape with a sharp interface and diameter D, the electron density here differs by $\Delta\rho$ from the average density. These regions are distributed randomly in the system, but the nearest neighbours do not come inside a distance R^*. The outside region possesses an electron density of $-\Delta\rho_n$, as shown in the figure. Owing to the randomness and the averaging at long distance, the electron density fluctuation decreases exponentially as a function of radial distance. Since a negative correlation was not observed, as shown in Fig. 9, $\Delta\rho_n$ is assumed to be zero. The above argument is expressed as follows:

$$\begin{aligned}\Delta\rho(r) &= \Delta\rho \qquad \text{for } -D/2 \leqslant r \leqslant D/2 \\ &= 0 \qquad \text{for } |r| > D/2\end{aligned} \tag{6}$$

$$\begin{aligned}\sum_k \sum_{j \neq k} \Delta\rho(r_{k1} + r + R_k - R_j) \\ = N\,\Delta\rho\, A \exp\left[-K_1(r_1 + r)\right] \text{ for } |r_1 + r| > R^* \\ = 0 \quad \text{for } -R^* < r_1 + r < R^*.\end{aligned} \tag{7}$$

Substituting Equations 6 and 7 into Equation 5, we obtain from the first term

$$\gamma_1(r) = N(\Delta\rho)^2 (D - r) \tag{8}$$

and from the second term:

$$\begin{aligned}\gamma_2(r) &= 0 \qquad \text{for } r \leqslant R^* - D/2 \\ &= \frac{N(\Delta\rho)^2 A}{K_1}\{\exp(-K_1 R^*) \\ &\quad - \exp\left[-K_1(r + D/2)\right]\} \\ &\qquad \text{for } R^* - D/2 < r \leqslant R^* + D/2 \\ &= \frac{N(\Delta\rho)^2 A}{K_1}[\exp(K_1 D/2) \\ &\quad - \exp(-K_1 D/2)] \exp(-K_1 r) \\ &\qquad \text{for } R^* + D/2 \leqslant r.\end{aligned} \tag{9}$$

The schematic representation of Equations 8 and 9 is drawn in Fig. 10b. The curves obtained characterize the feature presented in Fig. 9 well. Therefore the experimental data can be analysed by using the expressions of Equations 8 and 9 to obtain some structural parameters. The resulting

TABLE II Summary of the structure analysis of an Fe–17 at % B amorphous alloy, where the specimens were aged at 546 K for the time indicated

Ageing time	D (nm)	$N(\Delta\rho)^2$	$R^* + \frac{1}{2}D$ (nm)	A	K_1 (nm^{-1})
As-received	1.2	1.3	1.8	0.36	0.051
600 sec	0.9	2.2	2.05	0.14	0.052
3 ksec	0.9	2.2	2.45	0.15	0.056
30 ksec	1.0	2.0	2.4	0.18	0.060
300 ksec	1.0	2.0	2.4	0.18	0.060

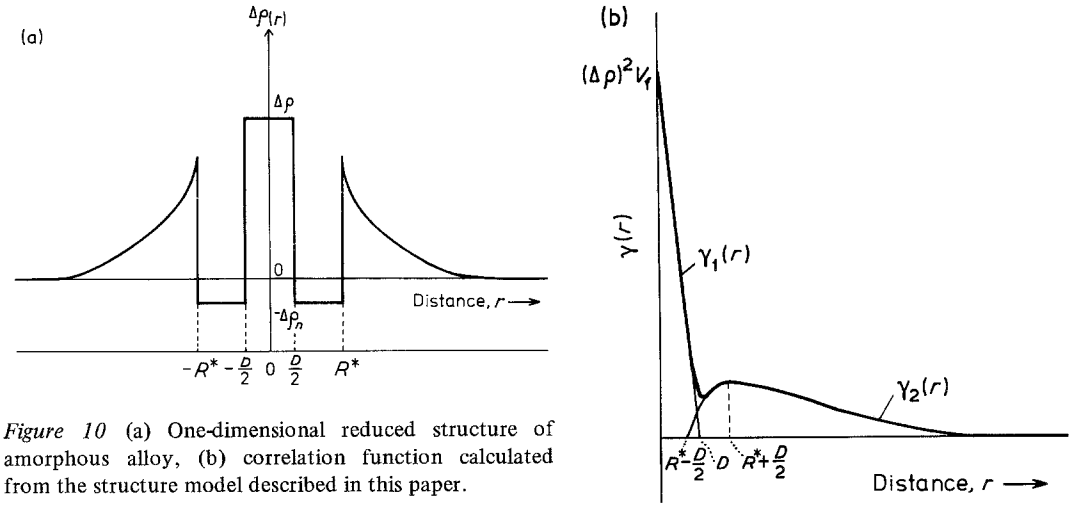

Figure 10 (a) One-dimensional reduced structure of amorphous alloy, (b) correlation function calculated from the structure model described in this paper.

values are listed in Table II, where $R^* + D/2$ is a nearest neighbour distance. For the as-received specimen, for example, the diameter of the fluctuating region is 1.2 nm and the nearest neighbour distance is 1.8 nm. This means that the electron density fluctuation occurs in a limited space. When the alloy was aged, the diameter decreased and the nearest neighbour distance increased for a short ageing period, but then remained nearly constant during further ageing. The exponential term in Equation 7 indicates the randomness of an arrangement of small regions contributing to SAXS intensity. The larger value of K_1 means that the randomness increases. During isothermal ageing, K_1 increased gradually. Yet the integrated intensity did not change much during isothermal ageing compared with that of the as-received state.

From the above analysis, one can state that $\Delta\rho$ is small in the as-received state, but the volume fraction occupied by the corresponding small regions is large, whereas during ageing for a short period, $\Delta\rho$ increases, but the volume fraction decreases and the atomic structure tends to go to a metastable state. The origin of those electron density fluctuations can be explained as indicated below.

As mentioned in Section 1, observed SAXS intensities correspond to the existence of electron density fluctuations in the amorphous state. The fluctuations could result from two alternative structural inhomogeneities, namely, compositional or density fluctuations. Boudreaux [2] suggested that amorphous alloys have a dual structure of well-defined molecular units and others. Our present experimental data seems to match his analysis. When a molecular unit with the composition of Fe_3B is formed and the units pack together to form a glass structure and the Fe atoms fill a space between units, the structural parameters are calculated as follows. Fe_3B has the same crystal structure as Fe_3C (cementite) [12]. The specific weight is assumed to be 7.27 g cm^{-3} [3, 5]. The electron density, ρ_{Fe_3B}, is calculated to be 2.036×10^{24} eu cm^{-3}. For α-iron, the electron density, ρ_{Fe}, and specific weight, d_{Fe}, are 2.207×10^{24} eu cm^{-3} and 7.87 g cm^{-3}, respectively. Then, for a $Fe_{83}B_{17}$ amorphous alloy, the parameters could be expected to be $\bar{d} = 7.49$ g cm^{-3}, the volume fraction $V_f = 0.355$, and

$$\gamma(0) = 0.0067 \times 10^{48} \text{ eu cm}^{-6}. \quad (10)$$

The calculated value of $\bar{d}$ is consistent with the observed value of 7.47 reported by Ray *et al.* [5].

For the as-received specimen, the experimental value of the integrated intensity is obtained by taking account of a Laue monotonic scattering. In the alloy system, the Laue monotonic scattering is always accompanied. Assuming that B atoms are located interstitially in a supposed supersaturated Fe–B solid solution of b c c structure and the lattices are divided into two types of unit cell, with and without B atoms, the Laue monotonic scattering intensity might be expressed as:

$$I_L(s) = x_{Fe}x_{Fe,B}(f_{Fe,B} - f_{Fe})^2/v_a, \quad (11)$$

where $f_{Fe,B}$ and f_{Fe} are nominal atomic scattering factors for the respective units, $x_{Fe,B}$ and x_{Fe} are mole fractions and v_a is an average molar volume. For a $Fe_{83}B_{17}$ alloy, the smeared intensity for the

Laue monotonic scattering is expressed by the chain-dotted line in Fig. 8. This indicates the intensity for a hypothetical supersaturated alloy. The Laue monotonic intensity for a phase-separated alloy is the sum of contributions from each phase, for which the intensity is given as in Equation 11, and is always lower than the above estimated hypothetical intensity. It is reasonable that the maximum Laue monotonic intensity is assumed to be given by the broken line in Fig. 8 for an as-received specimen, because no compositional fluctuation less than 1 nm exists in the system. Then the integrated intensity was calculated to be 0.0047×10^{48} eu cm^{-6} by substracting the contribution of the Laue monotonic scattering discussed here. This observed integrated intensity has the same order of magnitude as the theoretical value given by Equation 10, but is lower by about 42%. This indicates that phase separation does not go so far as a complete dual structure of Fe_3B/Fe, even though a compositional fluctuation exists in an amorphous Fe–B alloy. Further quantitative discussion on the amorphous structure, however, should be put in terms of a more strict three-dimensional structure model.

4. Conclusions

The variation in electrical resistivity during isothermal ageing was found to be a good measure of crystallization. Prior to the distinct crystallization of supersaturated b c c iron, a small change in electrical resistivity was observed, corresponding to the increase of SAXS intensity before any crystalline particles were detected by TEM observation. By using the interpretation of electrical resistivity reported by Landauer, the temperature dependence of resistivity for partially aged amorphous alloys was analysed. The volume fraction of the second phase estimated from the above analysis was in good agreement with the results of TEM observations.

The structure of an $Fe_{83}B_{17}$ amorphous alloy was examined in detail, mainly by means of SAXS measurements. An electron density fluctuation was observed in the amorphous alloy. The electron density–density correlation was derived from the observed intensity. The strong correlation was concentrated in a short radial distance within about 1.2 nm and the rather weak correlation extended further. These characteristic features were analysed on the basis of a two phase model. It is suggested that a compositional fluctuation occurs in a fine scale of about 1 nm in the amorphous Fe–B alloys. During isothermal ageing at low temperature, such a compositional fluctuation changed as a function of ageing time.

Acknowledgement

The authors wish to thank Associate Professor Dr H. P. Shingu for his valuable discussions.

Appendix

There are N particles in the unit volume and each particle possesses a centre of symmetry. Let r_{k1} be a vector to a position 1 from the centre of the kth particle and $\rho(r_{k1})$ be the electron density in an infinitesimal volume dv_1 around the position 1. Then the scattering amplitude from the system is expressed by

$$\Psi(s) = \sum_{k=1}^{N} \int_{v_k} \rho(r_{k1}) \exp\left[-i\,s(R_k + r_{k1})\right] dr_1, \tag{A1}$$

where R_k is the vector showing the centre of the kth particle. The scattering intensity is given by

$$\begin{aligned} I(s) = N \int\int \rho(r_1)\,\rho(r_m) \exp\left[-i\,s(r_1 - r_m)\right] \\ \times dr_1\,dr_m + \sum_{k}^{N} \sum_{j\neq k}^{N-1} \exp\left[-i\,s(R_k - R_j)\right] \\ \times \int_{v_k}\int_{v_j} \rho(r_{k1})\,\rho(r_{jm}) \exp\left[-i\,s(r_{k1} - r_{jm})\right] \\ \times dr_1\,dr_m. \end{aligned} \tag{A2}$$

Here some variables are changed as follows,

$$R_j + r_{jm} = R_k + r_{k1} + r \tag{A3}$$

and

$$\rho(r) = \rho_0 + \Delta\rho(r), \tag{A4}$$

where ρ_0 is the average electron density over the system. Then the scattering intensity is deformed as

$$\begin{aligned} I(s) = \rho_0^2 V N^2 \int_v \exp(isr)\,dr + N \int_v \exp(isr) \\ \times \left[\int_v \Delta\rho(r_1)\,\Delta\rho(r_1 + r)\,dr_1\right] dr \\ + \int_v \exp(isr) \left[\sum_{k} \sum_{j\neq k} \int_v \Delta\rho(r_{k1}) \right. \\ \left. \times \Delta\rho(r_{k1} + r + R_k - R_j)\,dr_{k1}\right] dr, \end{aligned} \tag{A5}$$

where the first term is the scattering from the whole system and both the second and third terms contribute to the SAXS intensity. As discussed in our previous paper [1], the electron density–density correlation function per unit volume is given by Equation 5 in the text.

References

1. K. OSAMURA, K. SHIBUE, P. H. SHINGU and Y. MURAKAMI, *J. Mater. Sci.* **14** (1979) 945.
2. D. S. BOURDREAUX, *Phys. Rev. B* **18** (1978) 4039.
3. J. J. GILMAN, *Phil. Mag.* **B37** (1978) 577.
4. T. KEMENY, I. VINCZE and B. FOGARASSY, *Phys. Rev. B* **20** (1979) 476.
5. R. RAY, R. HASEGAWA, C-P. CHOU and L. A. DAVIS, *Scripta Metall.* **11** (1977) 973.
6. H. HIROYOSHI, K. FUKAMICHI, M. KIKUCHI, A. HOSHI and T. MASUMOTO, *Phys. Lett.* **65A** (1978) 163.
7. K. FUKAMICHI, M. KIKUCHI, S. ARAKAWA and T. MASUMOTO, *Solid State Commun.* **23** (1977) 955.
8. T. FUKUNAGA, M. MISAWA, K. FUKAMICHI, T. MASUMOTO and K. SUZUKI, Proceedings of the 3rd International Conference on Rapidly Quenched Metals **2** (1979) p. 325.
9. J. L. WALTER, S. F. BARTRAM and I. MELLA, Technical Information Series, General Electric Co., 78CRD105 (1978) p. 1.
10. R. LANDAUER, *J. Appl. Phys.* **23** (1952) 779.
11. D. C. WALLANCE, P. H. SIDLES and G. C. DANIELSON, *ibid.* **31** (1960) 168.
12. W. K. CHOO and R. KAPLOW, *Met. Trans.* **8A** (1977) 417.

Received 10 July and accepted 4 September 1980.